J|A|C|S
ARTICLES

Published on Web 10/05/2009

Excited States Decay of the A−T DNA: A PCM/TD-DFT Study in Aqueous Solution of the (9-Methyl-adenine)$_2$·(1-methyl-thymine)$_2$ Stacked Tetramer

F. Santoro,[†] V. Barone,[‡] and R. Improta*[,§,||]

Istituto per i Processi Chimico-Fisici - CNR, Area della Ricerca del CNR Via Moruzzi, 1 I-56124 Pisa, Italy, Scuola Normale Superiore di Pisa, P.zza dei Cavalieri 7, I-56126 Pisa, Italy, Dipartimento di Chimica and INSTM, Università Federico II, Complesso Monte S. Angelo, via Cintia, I-80126 Napoli, Italy, and Istituto di Biostrutture e Bioimmagini - CNR, Via Mezzocannone 16, I-80134 Napoli, Italy

Received June 11, 2009; E-mail: robimp@unina.it

Abstract: By exploiting some of the most recent advances in the quantum mechanical methods, we have been able to analyze the behavior of the lowest energy excited states of A−T B-DNA using a realistic model, namely a double strand tetramer formed by two thymine−adenine stacked pairs in aqueous solution. The equilibrium structure of the lowest energy bright and dark excited states has been determined and their main properties disclosed. On this ground, our study provides a detailed atomistic picture of the excited state decay and of the emission process, and it highlights the specific roles of base stacking and pairing. While absorption involves excited states delocalized over different stacked bases, emission mainly takes place from individual monomers and it is dominated by thymine bases. We show that fast "monomer-like" excited state decay routes are operative also in the double strand. On the other hand, the long living components of the excited state population of (dA)·(dT) oligomers correspond to a dark excimer produced by intermonomer charge transfer between two stacked adenine bases, whereas adenine−thymine proton transfer plays a minor role in the excited state decay.

1. Introduction

DNA strongly absorbs solar ultraviolet light and many DNA photolesions are triggered by the population of singlet excited electronic states. The existence of fast and efficient nonradiative decay routes from these states is thus fundamental to life, but their nature is not yet completely understood. As a consequence, in the past decade, several extensive investigations of the dynamical properties of the photoexcited states of DNA and of its constituents[1−23] have appeared in the literature.

Although several important details (such as, for instance, the role played by dark excited states)[2,3] still wait for a definitive assessment, the excited state decay routes in isolated nucleobases can nowadays be considered sufficiently understood.[1] Indeed, ultrafast time-resolved experiments have shown that the bright excited states of purine and pyrimidine bases have subps lifetimes.[1,2] Computational studies have in fact identified barrierless paths connecting the Franck−Condon (FC) region

[†] Istituto per i Processi Chimico-Fisici - CNR.
[‡] Scuola Normale Superiore di Pisa.
[§] Università Federico II.
[||] Istituto di Biostrutture e Bioimmagini - CNR.

(1) Crespo-Hernandez, C. E.; Cohen, B.; Hare, P. M.; Kohler, B. *Chem. Rev.* **2004**, *104*, 1977–2020.
(2) Middleton, C. T.; de La Harpe, K.; Su, C.; Law, Y. K.; Crespo-Hernadez, C. E.; Kohler, B. *Annu. Rev. Phys. Chem.* **2009**, *60*, 13–47.
(3) Hare, P. M.; Crespo-Hernandez, C. E.; Kohler, B. *Proc. Natl. Acad. Sci. U.S.A.* **2007**, *104*, 435–441.
(4) Crespo-Hernández, C. E.; Cohen, B.; Kohler, B. *Nature* **2005**, *436*, 1141–1144.
(5) Schwalb, N. K.; Temps, F. *Science* **2008**, *322*, 243–245.
(6) Schreier, W. J.; Schrader, T. E.; Koller, F. O.; Gilch, P.; Crespo-Hernández, C. E.; Swaminathan, N.; Carell, T.; Zinth, W.; Kohler, B. *Science* **2007**, *315*, 625–629.
(7) Schultz, T.; Samoylova, E.; Radloff, W.; Hertel, I. V.; Sobolewski, A. L.; Domcke, W. *Science* **2004**, *306*, 1765–1768.
(8) Crespo-Hernandez, C. E.; Kohler, B. *J. Phys. Chem. B* **2004**, *108*, 11182–11188.
(9) Sobolewski, A. L.; Domcke, W.; Hattig, C. *Proc. Natl. Acad. Sci. U.S.A.* **2005**, *102*, 17903–17906.
(10) Buchvarov, I.; Wang, Q.; Raytchev, M.; Trifonov, A.; Fiebig, T. *Proc. Natl. Acad. Sci. U.S.A.* **2007**, *104*, 4794–4797.
(11) Tonzani, S.; Schatz, G. C. *J. Am. Chem. Soc.* **2008**, *130*, 7607–7612.
(12) Takaya, T.; Su, C.; de La Harpe, K.; Crespo-Hernández, C. E.; Kohler, B. *Proc. Natl. Acad. Sci. U.S.A.* **2008**, *105*, 10285–10290.
(13) Markovitsi, D.; Talbot, F.; Gustavsson, T.; Onidas, D.; Lazzarotto, E.; Marguet, S. *Nature* **2006**, *441*, E7.
(14) Markovitsi, D.; Onidas, D.; Gustavsson, T.; Talbot, F.; Lazzarotto, E. *J. Am. Chem. Soc.* **2005**, *127*, 17130–17131.
(15) Kwok, W.-M.; Ma, C.; Phillips, D. L. *J. Am. Chem. Soc.* **2006**, *128*, 11894–11905.
(16) Onidas, D.; Markovitsi, D.; Marguet, S.; Sharonov, A.; Gustavsson, T. *J. Phys. Chem. B* **2002**, *106*, 11367.
(17) Markovitsi, D.; Sharonov, A.; Onidas, D.; Gustavsson, T. *ChemPhysChem* **2003**, *3*, 303.
(18) Onidas, D.; Gustavsson, T.; Lazzarotto, E.; Markovitsi, D. *J. Phys. Chem. B* **2007**, *111*, 9644–9650.
(19) Markovitsi, D.; Gustavsson, T.; Talbot, F. *Photochem., Photobiol. Sci.* **2007**, *6*, 717.
(20) Banyasz, A.; Karpati, S.; Lazzarotto, E.; Markovitsi, D.; Douki, T. *J. Phys. Chem. C* **2009**, *113*, 11747–11750.
(21) Schwalb, N.; Temps, F. *J. Am. Chem. Soc.* **2007**, *129*, 9272–9273.
(22) Miannay, F.-A.; Banyasz, A.; Gustavsson, T.; Markovitsi, D. *J. Am. Chem. Soc.* **2007**, *129*, 14574–14575.
(23) Crespo-Hernandez, C. E.; de La Harpe, K.; Kohler, B. *J. Am. Chem. Soc.* **2008**, *130*, 10844–10845.

10.1021/ja904777h CCC: $40.75

with Conical Intersections (CoI) with the ground electronic state.[24−36]

The situation is much more involved in DNA single and double strands,[2] where time-resolved (TR) studies have revealed the existence of multiple decay channels, with very different time constants, often exhibiting a noticeable wavelength dependence, and spanning a range from hundreds of femtoseconds to hundreds of picoseconds (see Table 1).[4−19] As discussed in detail in the next sections, both Fluorescence Upconversion (FU) and Transient Absorption (TA) TR experiments show that in single and double DNA strands an ultrafast (lifetimes ≈ some hundreds of femtoseconds) decay is still present, whose behavior is similar to that exhibited by the isolated nucleobases (vide infra), suggesting the existence of "monomer-like" excited states and/or decay channels within polynucleotides.[4−19]

A lively debate still exists, instead, concerning the nature of the slower excited state decay channels, which are usually assigned to the so-called excimers,[37] evidenced in single and double strands and on the mechanisms responsible for their decay.[2−18] Several authors have suggested that the most important decay route is provided by base stacking. The observation[4] that the excited state decay in $(dA)_{18}\cdot(dT)_{18}$ is very similar to that found in $(dA)_{18}$ and that no long-living component is present in $(dT)_{18}$ suggests that most of excited state population decays to an intrastrand excimer formed by stacked adenines (A), whose features, as confirmed by our previous study on stacked A oligomers,[38,39] suggest a charge transfer (CT) character.[4] This hypothesis has received further support by another very recent study of Kohler et al.,[12] which shows that a long-living component (time constants in the range 10−100 ps) is present in several dinucleosides and that its lifetime is correlated to the stability of the interbase CT states. Serrano-Andrés et al., on the ground of a CASPT2 study of the A stacked dimer,[40] have instead suggested that the long-living components of the excited state decay are related to the formation of a "neutral" excimer (i.e., without any significant CT character) exhibiting maximum-overlap face-to-face orientations and short interbase distances (∼3 Å).

Table 1. Summary of the Most Important Time-Resolved Experimental Results on $(dA)_n\cdot(dT)_n$ System and Its Constituents[a]

FU experiments			
probe λ (nm)	τ_1 (ps)	τ_2 (ps)	τ_3 (ps)
	Adenosine-monophosphate (AMP)		
350 (ref 5)	0.27		
330 (ref 16)	0.1 (0.95)	0.52 (0.05)	
310−420 (ref 15)	0.13 (λ 307 nm[b])	0.45 (λ 344 nm[b])	
	thymine-monophosphate (TMP)		
350 (ref 5)	0.2	1.2	
330 (ref 16)	0.21(0.67)	1.07(0.33)	
		$(dA)_{20}$	
330 (ref 17)[b]	0.3(0.76)	1.6(0.22)	
350 (ref 5)	0.63(0.80)	5.80(0.13)	97 (0.07)
310−420 (ref 15)	0.39 (λ 310 nm[b])	4.3 (λ 348 nm[b])	182 (λ 390 nm[b])
		$(dT)_{20}$	
330 (ref 17)	0.3(0.64)	1.27 (0.32)	
350 (ref 5)	0.60(0.77)	2.96(0.23)	
		$(dA)_{20}\cdot(dT)_{20}$	
330 (ref 17)	0.4(0.56)	2.4(0.42)	
350 (ref 5)	0.52(0.41)	2.60(0.53)	16.2 (0.07)
310 (ref 18)	0.34 (0.78)	2.24 (0.22)	
330 (ref 18)	0.46 (0.66)	2.80 (0.34)	
380 (ref 18)	0.48 (0.76)	3.83 (0.24)	
420 (ref 18)	0.52 (0.81)	6.08 (0.19)	

TA experiments			
probe λ (nm)	τ_1 (ps)	τ_2 (ps)	τ_3 (ps)
		AMP	
250 (ref 4)		2.02(1.00)	
280 (ref 4)	0.33(1.00)		
570 (ref 4)	0.33(1.00)		
		TMP	
253 (ref 4)		2.38(0.86)	103 (0.11)
280 (ref 4)	0.74(0.62)	2.38(0.33)	
570 (ref 4)	0.74(1.00)		
		$(dA)_{18}$	
570[c] (ref 8)	1.33(0.29)		154 (0.64)
250 (ref 4)		2.0(0.63)	126 (0.34)
280 (ref 4)	0.33(0.84)	2.02(0.15)	126 (0.01)
360 (ref 4)		5.0(0.65)	126 (0.34)
570 (ref 4)	0.80(0.55)		126 (0.41)
		$(dT)_{18}$	
253 (ref 4)		2.38(0.79)	103 (0.14)
280 (ref 4)	0.74(0.62)	2.38(0.33)	
570 (ref 4)	0.74(1.00)		
		$(dA)_{18}\cdot(dT)_{18}$	
250 (ref 4)		2.46(0.71)	101 (0.25)
570 (ref 4)	1.1(0.52)		101 (0.34)

[a] Time-constant associated to the different components of the decay and their weights in the exponential fit (in parentheses) are reported. [b] The emission maximum of each component is reported. [c] On poly(dA).

(24) (a) Matsika, S. *J. Phys. Chem. A* **2004**, *108*, 7584–7590. (b) Serrano-Perez, J. J.; Gonzalez-Luque, R.; Merchán, M.; Serrano-Andrés, L. *J. Phys. Chem. B* **2007**, *111*, 11880–11883. (c) Merchán, M.; Gonzalez-Luque, R.; Climent, T.; Serrano-Andrés, L.; Rodriguez, E.; Reguero, M.; Pelez, D. *J. Phys. Chem. B* **2006**, *110*, 26471. (d) Perun, S.; Sobolewski, A. L.; Domcke, W. *J. Phys. Chem. A* **2006**, *110*, 13238. (e) Hudock, H. R.; Levine, B. G.; Thompson, A. L.; Satzger, H.; Townsend, D.; Gador, N.; Ullrich, S.; Stolow, A.; Martinez, T. J. *J. Phys. Chem. A* **2007**, *111*, 8500. (f) Zgierski, M. Z.; Patchkovskii, S.; Fujiwara, T.; Lim, E. C. *J. Phys. Chem. A* **2005**, *109*, 9384–9387. (g) Zechmann, G.; Barbatti, M. *J. Phys. Chem. A* **2008**, *112*, 8273–8279.

(25) Epifanovsky, E.; Kowalski, K.; Fan, P.-D.; Valiev, M.; Matsika, S.; Krylov, A. I. *J. Phys. Chem. A* **2008**, *112*, 9983–9992.

(26) (a) Ismail, N.; Blancafort, L.; Olivucci, M.; Kohler, B.; Robb, M. A. *J. Am. Chem. Soc.* **2002**, *124*, 6818–6819. (b) Merchán, M.; Serrano-Andrés, L.; Robb, M. A.; Blancafort, L. *J. Am. Chem. Soc.* **2005**, *127*, 1820–1825.

(27) (a) Serrano-Andrés, L.; Merchán, M.; Borin, A. C. *Proc. Natl. Acad. Sci. U.S.A.* **2006**, *103*, 8691–8696. (b) Serrano-Andrés, L.; Merchán, M.; Borin, A. C. *Chem.−Eur. J.* **2006**, *12*, 6559.

(28) Marian, C. M. *J. Chem. Phys.* **2005**, *122*, 104314.

(29) (a) Serrano-Andrés, L.; Merchán, M.; Borin, A. C. *J. Am. Chem. Soc.* **2008**, *130*, 2473. (b) Chen, H.; Li, S. H. *J. Chem. Phys.* **2006**, *124*, 154315. (c) Yamazaki, S.; Domcke, W. *J. Phys. Chem. A* **2008**, *112*, 7090–7097. (d) Shukla, M. K.; Leszczynski, J. *J. Phys. Chem. B* **2008**, *112*, 5139–5151. (e) Marian, C. M. *J. Phys. Chem. A* **2007**, *111*, 1545–1553.

(30) Improta, R.; Barone, V. *J. Am. Chem. Soc.* **2004**, *126*, 14320.

(31) Gustavsson, T.; Banyasz, A.; Lazzarotto, E.; Markovitsi, D.; Scalmani, G.; Frisch, M. J.; Barone, V.; Improta, R. *J. Am. Chem. Soc.* **2006**, *128*, 607–619.

(32) Santoro, F.; Barone, V.; Gustavsson, T.; Improta, R. *J. Am. Chem. Soc.* **2006**, *128*, 16312–16322.

(33) Gustavsson, T.; Sarkar, N.; Lazzarotto, E.; Markovitsi, D.; Barone, V.; Improta, R. *J. Phys. Chem. B* **2006**, *110*, 12843–12847.

(34) Mercier, Y.; Santoro, F.; Reguero, M.; Improta, R. *J. Phys. Chem. B* **2008**, *112*, 10769–10772.

(35) Improta, R.; Barone, V. *Theor. Chem. Acc.* **2008**, *120*, 491–497.

(36) Karunakaran, V.; Kleinermanns, K.; Improta, R.; Kovalenko, S. A. *J. Am. Chem. Soc.* **2009**, *131*, 5839–5850.

(37) Eisinger, J.; Guéron, M.; Shulman, R. G.; Yamane, T. *Proc. Natl. Acad. Sci. U.S.A.* **1966**, *55*, 1015–1020.

(38) Santoro, F.; Barone, V.; Improta, R. *Proc. Natl. Acad. Sci. U. S. A.* **2007**, *104*, 9931–9937.

(39) Improta, R. *Phys. Chem. Chem. Phys.* **2008**, *10*, 2656–2664.

(40) Olaso-Gonzalez, G.; Merchán, M.; Serrano-Andrés, L. *J. Am. Chem. Soc.* **2009**, *131*, 4368–4377.

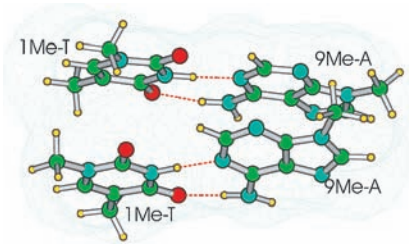

Figure 1. Schematic drawing of the $(9Me\text{-}A)_2\cdot(1Me\text{-}T)_2$, adopting the B-DNA conformation, investigated in the present study. The cavity used for modeling solvent effect by PCM is also shown.

Alternatively, base pairing has been proposed to rule the nonradiative decay, allowing proton transfers (PT) that ultimately lead to the ground state (S_0) recovery.[7,9] The experimental results obtained on the cytosine−guanine dimer in nonpolar solution support this model,[21] which, however, has been recently criticized.[22,23] To complete this short overview, we highlight that some researchers have questioned the existence itself of a unique dominant decay mechanism.[13,18]

It is clear that the mechanism underlying the decay of the excited states within single and, especially, double strand cannot be considered assessed. Experiments have allowed an impressive advance, but they often provide quite indirect information about the microscopic nature of the excited electronic states involved in the DNA interaction with the UV radiation. More in general, a comprehensive and detailed description of photoexcited DNA behavior, from absorption to emission, is still lacking. For example, several experiments indicate that the excited states involved in the absorption process are delocalized over multiple stacked bases.[10,11] On the other hand, on the ground of the strong similarity exhibited at earlier times by the fluorescence decay of $(dA)_{20}$ and of dA, it has been proposed that even the absorption process is localized on single A bases.[15]

First principle theoretical models could in principle provide fundamental insights, but their practical application is hampered by the remarkable dimension of the smallest realistic model of DNA, that is, a tetramer being able to describe both inter and intrastrand interactions. Furthermore, a proper account of the solvent effect is very important for a direct comparison between experiments and calculations and it is mandatory for a reliable treatment of electronic transitions with partial CT character.

Exploiting the latest advances in the density functional theory (DFT) and in its time-dependent (TD)[41,42] extension for electronic excited states, and in the Polarizable Continuum solvation Model (PCM),[43] we thus decided to study in detail the excited states of DNA double helix, focusing on A−T DNA, for which several complementary experimental studies exist.

In a preliminary contribution, we have studied by means of PCM/TD-DFT calculations the absorption spectrum in aqueous solution of $(dA)_2\cdot(dT)_2$ and of $(9Me\text{-}A)_2\cdot(1Me\text{-}T)_2$ (9Me-A = 9,methyl-adenine; 1Me-T = 1,methyl-thymine, see Figure 1) tetramer adopting the B-DNA structure.[44] As briefly discussed below, we have shown that our computational approach is able to reproduce the most important features of the double strand absorption spectra, when compared to those of the isolated monomers.

It is however clear that, to shed light on the excited state dynamics in DNA double helix, it is mandatory to locate the minima of the lowest energy excited states, to characterize their properties, and to analyze their behavior in the region of the PES connecting the minima with the FC region.

The above tasks are tackled in the present study. Focusing for the first time, to the best of our knowledge, on a realistic model of A−T DNA, that is, the $(9Me\text{-}A)_2\cdot(1Me\text{-}T)_2$ tetramer, an atomistic picture of the lowest-energy A−T DNA excited electronic states and of their equilibrium structures is obtained, assessing the effect of interstrand hydrogen bonding and intrastrand base stacking. Our results provide very strong indications that base-stacking is the key factor ruling the excited state decay and that the slow time components are due to CT states involving stacked adenine bases.

Three different hybrid functionals have been adopted in our PCM/TD-DFT calculations to ensure that the conclusions are not biased by ad hoc choices. Apart from the widely used parameter free PBE0 functional,[45] we employed the M052X[46] and the CAM-B3LYP functionals,[47] which are particularly effective for treating stacked molecules and CT transitions.[46] Solvent effects, whose inclusion is mandatory, especially for a reliable description of CT transitions, have been taken into account by the PCM also exploiting the very recent State Specific (SS) version of PCM/TD-DFT, which in several systems have already provided a very accurate description of solvent effects on the excited state behavior.[50,51]

2. Computational Details

The geometry of the adenine−thymine double strand has been extracted from the experimental structure of PolydeoxyAdenosine·PolydeoxyThyimine (1PLY.pdb) DNA double strand. In the geometry optimizations of the tetramer, all of the intramolecular and intermolecular degrees of freedom were fully unconstrained, with the exception of interbase distance and mutual orientation of the stacked bases that were kept frozen to their experimental values. However, we have previously checked that fully unconstrained geometry optimization does not significantly affect the computed absorption spectra.[44] Our analysis has been performed by using the parameter free PBE0,[45] which has already provided a very accurate description of the bright states of nucleobases,[30−36,38,39] providing vertical excitation and emission energies within ∼0.15 eV of the corresponding experimental absorption maxima. On the other hand, like many of the "standard" density functionals, PBE0 might overestimate the stability of long-range CT transitions.[39,52,53] As a consequence, our study has been performed by using two

(41) Dreuw, A.; Head-Gordon, M. *Chem. Rev.* **2005**, *105*, 4009–4037.
(42) Burke, K.; Werschnik, J.; Gross, E. K. U. *J. Chem. Phys.* **2005**, *123*, 062206.
(43) Tomasi, J.; Mennucci, B.; Cammi, R. *Chem. Rev.* **2005**, *105*, 2999–3094.
(44) Santoro, F.; Barone, V.; Improta, R. *ChemPhysChem* **2008**, *9*, 2531–2537.
(45) (a) Adamo, C.; Barone, V. *J. Chem. Phys.* **1999**, *110*, 6158–6170. (b) Enzerhof, M.; Scuseria, G. E. *J. Chem. Phys.* **1999**, *110*, 5029. (c) Adamo, C.; Scuseria, G. E.; Barone, V. *J. Chem. Phys.* **1999**, *111*, 2889–2899.
(46) (a) Zhao, Y.; Truhlar, D. G. *Acc. Chem. Res.* **2008**, *41*, 157–167. (b) Zhao, Y.; Schultz, N. E.; Truhlar, D. G. *J. Chem. Theory Comput.* **2006**, *2*, 364.
(47) (a) Yanai, T.; Tew, D. P.; Handy, N. C. *Chem. Phys. Lett.* **2004**, *393*, 51–55. (b) Tawada, Y.; Tsuneda, T.; Yanagisawa, S.; Yanai, T.; Hirao, K. *J. Chem. Phys.* **2004**, *120*, 8425.
(50) Improta, R.; Barone, V.; Scalmani, G.; Frisch, M. J. *J. Chem. Phys.* **2006**, *125*, 054103.
(51) Improta, R.; Frisch, M. J.; Scalmani, G.; Barone, V. *J. Chem. Phys.* **2007**, *127*, 74504.
(52) Lange, A. W.; Rohrdanz, M. A.; Herbert, J. M. *J. Phys. Chem. B* **2008**, *112*, 6304.
(53) Lange, A. W.; Herbert, J. M. *J. Am. Chem. Soc.* **2009**, *131*, 3913–3922.

additional density functionals, namely M052X, which is particularly effective for the treatment of stacked molecules[46] and CAM-B3LYP, which has been tailored in order to accurately treat long-range CT transitions. Both M052X and CAM-B3LYP are not biased (see ref 39 and Supporting Information) by the traditional failure of TD-DFT[41,42] in the treatment of CT transitions. Whenever not explicitly stated, ground state geometry optimizations have been performed in aqueous solution at the PCM/PBE0/6-31G(d) level, including bulk solvent effects by the polarizable continuum model (PCM).[43]

Excited state geometry optimizations in solution have been performed by using the "standard" LR (linear-response) implementation of PCM/TD-DFT,[54] for which analytical gradients are available.[55] LR-PCM/TD-DFT computes excitation energies directly, without using the true excited state electron density. Our previous studies indicate that this implementation provides an accurate estimate of solvent effect on bright transitions and reliable excited state equilibrium geometries.[48,49] We also resorted to the recently developed State-Specific (SS) implementation of PCM/TD-DFT.[50,51] In SS approaches, a fully variational formulation of the solvent effect on the excited state properties is achieved, by solving a different effective Shroedinger equation for each state of interest and thus providing a more balanced description of solvent effects on different excited electronic states than LR-PCM, especially when dealing with transitions (like the CT ones) involving large changes of the electron density.[50,51]

When discussing solvent effects on absorption spectra, it is useful to define two limit situations, usually referred to as nonequilibrium (*neq*) and equilibrium (*eq*) time-regimes.[43,56] In the former case, only solvent electronic polarization (fast solvent degrees of freedom) is in equilibrium with the excited state electronic density of the solute, whereas nuclear degrees of freedom (slow solvent degrees of freedom) are equilibrated with the ground state electron density. On the contrary, the equilibrium regime is reached when both fast and slow degrees of freedom are equilibrated with the excited state electron density. The solvent reaction field in the nonequilibrium regime depends in the PCM formalism on the dielectric constant at optical frequency (ε_{opt}, usually related to the square of the solvent refractive index n, $\varepsilon_{opt} = n^2$, for water 1.776). PCM equilibrium solvation is instead ruled by the static dielectric constant (ε, for water 78.39). To calculate the vertical excitation energies and to discuss the fast part of the excited state dynamics (time <200 fs) *neq* solvation energies are more suitable, whereas the *eq* time regime can better model the excited state energies for the slower part of the excited state dynamics (time >1 ps) and for the long-time fluorescence process.

The effect of basis set extension on AED (adiabatic energy differences) and VEE (vertical emission energies) has been estimated by test computations with more extended 6-31+G(d,p) and 6-311+G(2d,2p) basis sets. All of the calculations have been performed by a development version of the Gaussian Program.[57]

3. Results

3.1. Validation of our Computational Methodology. Model. Before starting the analysis of our results, it is important to verify not only the reliability of our computational approach but also the suitability of the model studied for interpreting the excited state dynamics in A−T DNA. In this respect, our study of the absorption spectra (see Supporting Information for a detailed discussion) strongly suggests that (9Me-A)$_2$·(1Me-T)$_2$ is a reliable model for studying the excited state dynamics of A−T DNA, especially on the ≤1 ps time-scale, that is critical for the process we are dealing with. Experiments[4] suggest indeed that the "excimer" state associated to the slow decay channel is formed within 1 ps after the excitation. On this time-scale, the excited state dynamics is expected to be ruled by intramolecular motions of the nucleobases.

To be sure that neglecting the phosphoribose backbone does not qualitatively affect our conclusion, we choose a very "conservative" approach. As anticipated above, in the excited state geometry optimizations the intramonomer distances and the relative orientation of the stacked bases have been kept frozen to that adopted in B-DNA, while all of the remaining degrees of freedom have been fully relaxed. From the dynamical point of view, the underlying assumption is that, upon photoexcitation, high frequency modes (intramolecular bond stretchings, bond bendings and out of plane motions) change faster than "low frequency" degrees of freedom as those involved in the stacking interaction. In any case, we highlight that in a previous paper[38] we have already shown that the relative stability of CT and bright excited states are not affected by small variation of the distance between two stacked monomers.

QM Method. As discussed in detail in the Supporting Information, the reliability of PCM/TD-PBE0 calculations in the study of the bright π/π^* and of the dark $n\pi^*$ excited states in the monomers can be considered assessed.[30−36] Furthermore, when dealing with the dimers or the tetramer, our approach is able to provide a good estimate of the effect of stacking and hydrogen bonding interactions on the excited state properties.[38,39,44] Additional considerations are instead necessary for what concerns the relative stability of transitions with significant CT character.

To assess the accuracy in describing interstrand charge transfer transitions we have optimized in the gas phase the (9Me-A)·(1Me-T) Watson−Crick hydrogen bonded pair, computing the lowest energy transitions by using different density functionals. Data in Table 2 show that M052X and CAM-B3LYP functionals predict that the A→T CT transition is less stable by ∼0.8 eV than the bright excited state localized on T. This result agrees within 0.15 eV with the predictions of ab initio CC2 methods.[53,58] For what concerns the CT transitions between stacked bases, the system to focus on is the stacked A dimer, since CT transitions between stacked thymine (T) are not significantly involved in the tetramer excited state dynamics (vide infra). The performances of different density functionals (PBE0, CAM-B3LYP, M052X, LC-ωPBE) have been examined in detail in a previous contribution.[39] We have shown that PBE0 overestimates the stability of intrastrand CT transitions, with respect to the other examined functionals, although the amount of the overestimation is smaller than what found for A−T interstrand CT transitions. In fact, the most dramatic failures of "standard" density functionals in treating CT transitions occur in the case of zero overlap between the MO's of the donor and the acceptor molecule.[41]

To compare our results with the available post-HF results, we have computed the absorption spectrum of (9Me-A)$_2$ in the

(54) Cossi, M.; Barone, V. *J. Chem. Phys.* **2001**, *115*, 4708–4717.
(55) Scalmani, G.; Frisch, M. J.; Mennucci, B.; Tomasi, J.; Cammi, R.; Barone, V. *J. Chem. Phys.* **2006**, *124*, 094107.
(48) Barone, V.; Improta, R.; Rega, N. *Acc. Chem. Res.* **2008**, *41*, 605–616.
(49) (a) Santoro, F.; Improta, R.; Lami, A.; Bloino, J.; Barone, V. *J. Chem. Phys.* **2007**, *126*, 084509. (b) Santoro, F.; Lami, A.; Improta, R.; Barone, V. *J. Chem. Phys.* **2007**, *126*, 184102.
(56) Cossi, M.; Rega, N.; Scalmani, G.; Barone, V. *J. Chem. Phys.* **2001**, *114*, 5691.
(57) Frisch, M. J.; et al. *Gaussian development version GDV*, version F.02; Gaussian Inc.: Wallingford, CT, 2006.
(58) Perun, S.; Sobolewski, A. L.; Domcke, W. *J. Phys. Chem. A.* **2006**, *110*, 9031.

Table 2. Adiabatic Energy Differences (AED, in eV) with Respect to the Ground State Minimum, Vertical Emission Energies (VEE, in eV), and Dipole Moment (in Debye) Computed for the $(9Me\text{-}A)_2 \cdot (1Me\text{-}T)_2$ Tetramer in Water[a]

$(9Me\text{-}A)_2 \cdot (1Me\text{-}T)_2$ tetramer in water - Excited State Minima					
	AED		VEE[e]		μ
	6-31G(d)	6-31+G(d,p)	6-31G(d)	6-31+G(d,p)	6-31G(d)
			PBE0		
AT_{CT}	4.58(0.00)[b]	4.54(0.00)[b]	4.23	4.17	16.7[f]
AA_{CT}	4.44(0.00)[b]	4.43(0.00)[b]	4.56		14.5
$A\text{-}S_B$[c]	4.85(0.20)	4.74(0.21)	4.35	4.33	5.50
$T\text{-}S_B$[d]	4.83(0.07)	4.70(0.08)	3.79	3.75	4.06
			M052X		
AT_{CT}	4.84(0.01)	4.81(0.01)	4.42	4.32	16.3
AA_{CT}	4.72(0.00)	4.72(0.00)	4.80	4.70	14.4
$A\text{-}S_B$[c]	5.16(0.26)	5.03(0.30)	4.58	4.57	5.60
$T\text{-}S_B$[d]	4.90(0.13)	4.83(0.12)	4.03	3.91	4.50
			CAM-B3LYP		
AT_{CT}	4.86(0.01)	4.79(0.01)	4.43	4.31	16.3
AA_{CT}	4.68(0.00)	4.68(0.00)	4.75	4.64	14.4
$A\text{-}S_B$[c]	5.06(0.25)	4.93(0.28)	4.62	4.48	5.60
$T\text{-}S_B$[d]	4.92(0.12)	4.84(0.12)	4.00	3.87	4.30

AED of $(9Me\text{-}A) \cdot (1Me\text{-}T)$ base-pair in the gas phase- FC point							
	PBE0		M052X		CAM-B3LYP		CC2/MP2[g]
	6-31G(d)	6-31+G(d,p)	6-31G(d)	6-31+G(d,p)	6-31G(d)	6-31+G(d,p)	
AT_{CT}	4.73(0.00)	4.57(0.00)	6.08(0.00)	5.92(0.00)	6.03(0.00)	5.84(0.00)	6.26(0.00)
$A\text{-}S_B$	5.21(0.18)	5.04(0.23)	5.56(0.28)	5.39(0.34)	5.44(0.20)	5.26(0.32)	5.45(0.25)
$T\text{-}S_B$	5.12(0.20)	4.92(0.20)	5.38(0.23)	5.18(0.24)	5.28(0.21)	5.07(0.23)	5.37(0.16)

AED of $(9Me\text{-}A)_2$ stacked dimer in the gas phase- FC point							
	PBE0		M052X		CAM-B3LYP		CC2[h]
	6-31G(d)	6-31+G(d,p)	6-31G(d)	6-31+G(d,p)	6-31G(d)	6-31+G(d,p)	
AA_{CT}	4.98(0.00)	4.86(0.00)	6.04(0.00)	5.90(0.00)	5.95(0.00)	5.76(0.00)	6.19
$A\text{-}S_B$	5.29(0.29)	5.12(0.25)	5.63(0.40)	5.45(0.20)	5.52(0.31)	5.33(0.18)	5.55

[a] Non-equilibrium state specific PCM/TD-DFT results according to PBE0, M052X, and CAM-B3LYP functionals on PCM/TD-PBE0/6-31G(d) optimized geometries. Oscillator strengths are also reported in parentheses. The AED computed in the gas phase for the $(9Me\text{-}A)\cdot(1Me\text{-}T)$ hydrogen bonded dimers (Watson and Crick pairing) are also reported. [b] Corrected for the overestimation of the stability of CT transitions. [c] $A\text{-}S_B$ stands for the pair of almost degenerate localized states $A1\text{-}S_B$ and $A2\text{-}S_B$. [d] $T\text{-}S_B$ stands for the pair of almost degenerate localized states $T1\text{-}S_B$ and $T2\text{-}S_B$. [e] LR-PCM results: the VEE of CT transitions is likely overestimated. [f] After PT the dipole moment is 3.7 D. [g] A−T dimer, ref 58. [h] Reference 53.

gas phase, by using the B-DNA like ground state minimum, optimized in aqueous solution, as reference geometry (see Table 2). CAM-B3LYP and M052X predicts that the lowest energy 9Me-A→9Me-A CT transition is ∼0.45 eV less stable than the excited states corresponding to the most intense electronic transition. This estimate is in good agreement with the 0.64 eV value provided by CC2/TZVP calculations on a similar system (two A molecules adopting the experimental B-DNA structure).[53] As anticipated above, PBE0 instead predicts that the CT transitions is ∼0.25 eV more stable than the bright excited state, with a smaller discrepancy with respect to the CC2 results than that found for the interstrand CT transition.

In aqueous solution, at the FC geometry, LR-PCM/TD-DFT/6-31G(d) calculations (using either CAM-B3LYP or M052X) predict that the lowest energy CT transition is ∼0.5 eV blue-shifted with respect to the maximum of the absorption band.[39] This prediction is in very good agreement with that obtained by Herbert et al. in their study using LC-ωPBE0 and LC-ωPBE0h functionals,[53] especially when the possible sources of error with respect to CC2 and CASPT2 benchmark calculations are considered in their computed spectra (see the SI of ref 53).

Solvent Model. A detailed discussion on the advantages and the drawbacks of the different approaches for including solvent effects on the computed absorption and fluorescence spectra it is obviously outside the scope of the present study (see Supporting Information for additional considerations).

Our experience in the field[48] indicate that continuum models and, when necessary, mixed discrete-continuum model, usually provide an accurate and reliable estimate of the solvent effect on the absorption and emission spectra.[43] For what concerns the isolated nucleobases, PCM/TD-PBE0 results are in excellent agreement (within 0.15 eV) with the available experimental absorption and emission maxima, providing accurate estimate of the Stokes Shift.[31,32,36] This latter point is very important, since an accurate estimation of the Stokes shift requires both an accurate determination of the excited state stationary points and a reliable treatment of dynamical solvation effects. On the other hand, we have previously shown that "conventional" LR-PCM approaches underestimate the relative stability of CT transitions with respect to the bright ones.[50,51] Furthermore LR-PCM cannot be considered a reference method for studying dynamical solvent effects.[50,51] Actually, a reliable treatment of CT states in solution also requires that their electronic density is properly described.[39] In this respect, state-averaging procedures, as those usually adopted in CASPT2/PCM calculations,

are not fully adequate to the study of absorption and emission processes involving electronic states with strongly different polarities.[59]

We have instead shown that a very accurate description of solvent effect on excited electronic states is provided by the recently developed State Specific implementation of PCM/TD-DFT.[50,51] For example, it is meaningful that SS-PCM/TD-PBE0 calculations are able to provide a very accurate description of the absorption and the emission properties of the lowest energy transition of coumarin C153, which exhibits a noticeable CT character.[60,61] On the balance, we can thus consider our SS-PCM/TD-DFT approach one of the most reliable, if not the most accurate, method for considering solvent effect on the properties of molecular systems in solution.

However, the (9Me-A)$_2$·(1Me-T)$_2$ tetramers are inserted in a DNA double helix. In this system, the response of the solvent nuclear degrees of freedom to the variation of the electron density associated to the electronic transitions is expected to be much slower than in a standard isotropic solvent, since it could involve also the motion of the bulky phosphate groups and of the counterions. As a consequence, to avoid any overestimation of solvent equilibration effects, we choose a conservative approach, and our conclusion will be based mainly on the *neq* results. This choice disfavors the excited states with a dipole moment significantly larger than that of the ground state (as the CT states) which are significantly stabilized by a full equilibration of solvent degrees of freedom.[39] As a consequence, we always computed the excited state energies also in the *eq* limit, to have insights on the possible role played by dynamical solvation effects.

In summary, the following analysis will be based mainly on TD-PBE0 computations, which have shown to provide a very accurate description of the bright state behavior, more reliable than that obtained by using long-range corrected density functionals.[39,44] On the other hand, PBE0 significantly overestimates the stability of CT transitions. Therefore, to avoid any artifact, in the present work the PBE0 CT states energies have been corrected on the ground of the M052X predictions, leading to a decrease of the relative stability of intrastrand CT states by ∼0.7 eV and of interstrand CT states by ∼1 eV. Specifically, the correcting energy shift has been estimated by comparing the relative stability of the CT states and the most intense transition localized on the A strand, predicted by LR-PCM/TD-PBE0/6-31G(d) and LR-PCM/TD-M052X/6-31G(d) calculations within the tetramer in solution at the FC point. In this way, we can indeed take into account any possible dependence of the CT overestimation on the specific features of the system studied.

It is not easy to quantify exactly the expected accuracy of our computational approach. On the balance, when compared to the available CC2 results, our analysis exhibits an accuracy comparable to that obtained by using LC-ωPBE and LC-ωPBEh functionals.[53] According to the analysis reported in ref 53, 0.3 eV should thus be a realistic, though prudential, estimate of the "confidence range" of our predictions.

3.2. Bright Excited States and Emission Spectrum. Figure 2 reports the absorption spectrum of our model system (9Me-A)$_2$·(1Me-T)$_2$ computed in aqueous solution at SS-PCM//TD-M052X/6-31G(d) level of theory.[44] The two lowest energy bright states in the Franck−Condon (FC) region are delocalized on the T strand (TT-S$_B$), and arise from the mixing of the lowest energy $\pi \rightarrow \pi^*$ transition in single T bases.[31] The absorption band maximum is instead mainly due to two excited states delocalized on the A strand (AA-S$_B$), deriving from the interaction between the singlet bright states localized on the two 9Me-A monomers[38] (see Supporting Information). Both for TT-S$_B$ and AA-S$_B$ pair of excited states, one state corresponds to an intense transition and the other to a weak one.

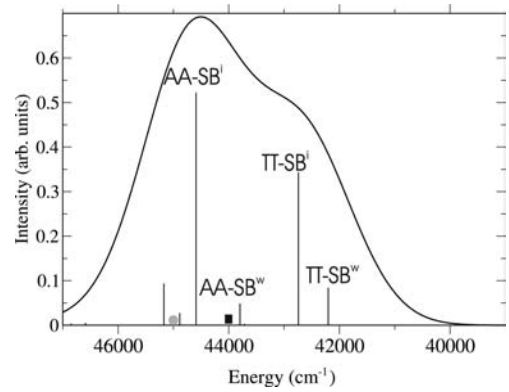

Figure 2. Convoluted and stick absorption spectrum of (9Me-A)$_2$·(1Me-T)$_2$, computed in aqueous solution at the PCM/TD-M052X/6-31G(d) level. i and w superscripts label strong and weak transitions, respectively. The position of the lowest energy CT transitions are also shown: AT$_{CT}$ (gray circle) and AA$_{CT}$ (black square).

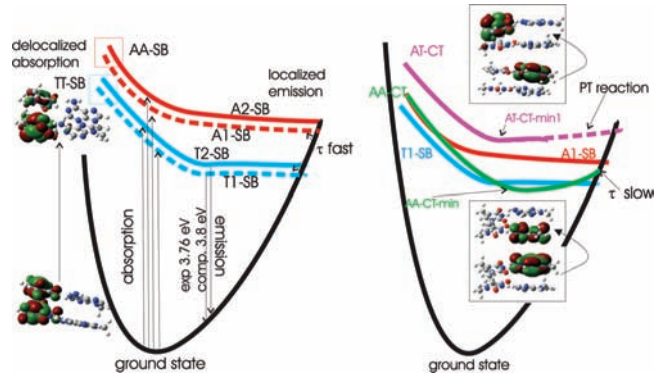

Figure 3. Pictorial description of the most significant processes involving (left) the bright excited states and (right) the dark excited states of (9Me-A)$_2$·(1Me-T)$_2$. As discussed in the text, a different reaction coordinate is associated to each excited state. A larger picture of the relevant molecular orbitals can be found in the Supporting Information.

By performing LR-PCM/TD-PBE0/6-31G(d) excited state geometry optimization, we have located the minima in aqueous solution of the four lowest energy bright excited states of (9Me-A)$_2$·(1Me-T)$_2$ adopting the B-DNA structure.

The main structural parameters of the bright states minima are given in Figure 4, while their AED with respect to the S$_0$ minimum are reported in Table 2. (Additional tables describing more in detail the electronic properties of the minima are reported in the Supporting Information, Tables S2−S5.)

Geometry optimizations of the TT-S$_B$ states lead to two different equilibrium structures (T1-S$_B$-min and T2-S$_B$-min), where the electronic transition (T1-S$_B$ and T2-S$_B$, respectively) is "localized" on a single monomer (see Figure 3). Specifically, one 1Me-T monomer exhibits a geometry very close to the S$_0$ minimum while the other one shows a structure similar to that

(59) Karlström, G.; Lindh, R.; Malmqvist, P.-A.; Roos, B. O.; Ryde, U.; Veryazov, V.; Widmark, P.-O.; Cossi, M.; Schimmelpfennig, B.; Neogrady, P.; Seijo, L. *Comput. Mater. Sci.* **2003**, *28*, 222–239.
(60) Improta, R.; Barone, V; Santoro, F. *Angew. Chem., Int. Ed.* **2007**, *46*, 405–408.
(61) Improta, R.; Barone, V.; Santoro, F. *J. Phys. Chem. B* **2007**, *111*, 14080.

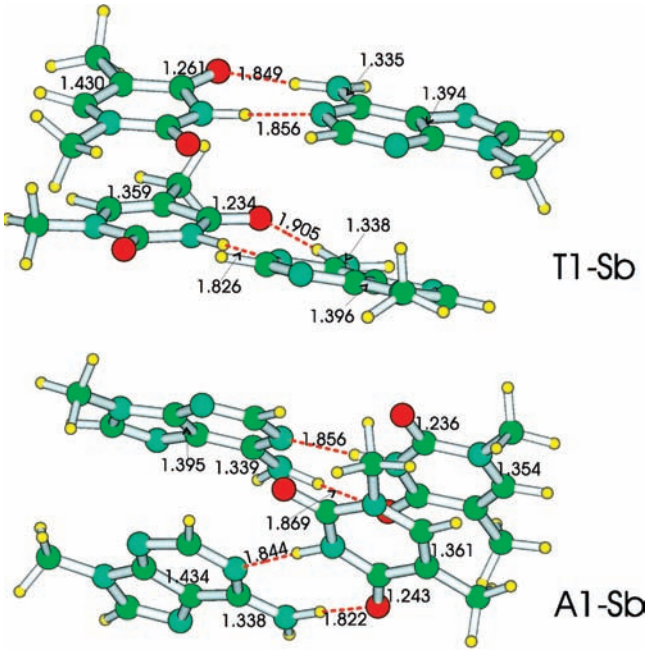

Figure 4. Schematic drawing and selected bond distances (in Å) of the $(9Me\text{-}A)_2\cdot(1Me\text{-}T)_2$ tetramer in the ground state minimum (top), in the minmium of T1-S_B (middle), and in the minimum of A1-S_B (bottom). Please note that the orientation of the tetramer is not the same in all of the Figures.

obtained by optimizing the lowest excited bright state of an isolated 1Me-T molecule. This involves a significant distortion from planarity of the pyrimidine ring that assumes a "boat-like" conformation. Not surprisingly, the largest variations of the bond lengths involve the lengthening of the C5−C6, C4−O8, and N3−C4 bond distances and the shortening of the C4−C5 bond distance, in line with the bonding/antibonding character of HOMO and LUMO with respect to those bonds (see Figure 4).

Although, due to the lack of symmetry of the stacking geometry in the double helix structure (i.e., the 5′ and the 3′ position of a stacked dimer are not perfectly equivalent), these two minima are not exactly isoenergetic, their energy difference is negligible (∼0.01 eV). 6-31+G(d,p) calculations indicate that the T1-S_B-min/T2-S_B-min AED is 4.7 eV, while their VEE is in the range 3.8−4.0 eV (depending on the adopted density functional).

The VEE values allow us to assign to this pair of states the experimental emission maximum, which falls at 3.76 eV for $(dA)_{20}\cdot(dT)_{20}$.[18] Our finding that the geometry and the energy of T1-S_B-min is very similar to that of isolated T explains why the experimental fluorescence spectrum of $(dA)_n\cdot(dT)_n$ is almost superimposable to that of dT.[18,19]

As for TT-S_B, geometry optimization of AA-S_B pair of states leads to two almost-degenerate excited state minima (A1-S_B-min/A2-S_B-min) corresponding to a "localized" transition on a single monomer (hereafter A1-S_B and A2-S_B, see Figure 4). One 9Me-A molecule has thus almost the same geometry of the ground state, whereas the other 9Me-A base exhibits the same changes found when optimizing the Ade-S_B state of an insulated 9Me-A molecules. The PBE0 VEE is ∼4.3 eV (see Table 2), close to the emission energy detected in dA, 4.05 eV[15] (the computed absorption maximum of DNA, due to A contributions, is also blue-shifted by ∼0.2 eV with respect to the experimental one).

After localization on a single monomer, it is reasonable to assume that A1-S_B can follow the same decay pathway highlighted for the bright states in isolated A.[27] Both experiments and computations indicate that this state is characterized by an ultrashort lifetime (∼100 fs).[15,27]

The very low fluorescence anisotropy evidenced by experiments[18] thus finds a rationale within the framework of our finding that absorbing and emitting states are different. Absorption is delocalized over multiple bases (up to 4−5).[10,11,38,39] Especially on the longer time scale, emission comes instead from several individual monomers through transitions polarized in planes perpendicular to the helical axis, which produce a limiting value of 0.1 for the fluorescence anisotropy,[18] that is, the value experimentally determined at 420 nm, 3 ps after the excitation, for $(dA)_{20}\cdot(dT)_{20}$.[18]

3.3. Dark Excited States. According to our calculations, several dark states fall in the same energy range of the bright transitions in $(9Me\text{-}A)_2\cdot(1Me\text{-}T)_2$,[44] and some of them have CT character (see Figure 2). The most stable CT state corresponds to the transfer of an electron between two stacked 9Me-A, AA_{CT} (as for the bright states, also in this case we should actually speak of a pair of almost degenerate states $A1A2_{CT}$ and $A2A1_{CT}$; this will be avoided for the sake of shortness). Geometry optimization of AA_{CT} leads to the stationary point AA_{CT}-min, exhibiting a clear-cut A→A CT character (see Figure 5), involving the transfer of ∼0.8 au (see Supporting Information). AA_{CT}-min exhibits a nuclear structure typical of a 9Me-$A^-\cdot$9Me-A^+ stacked pair. The geometries of two 9Me-A molecules are strongly different and closely resemble those of the 9Me-A radical cation and anion, respectively. For example the CN bond lengths involving the exocyclic NH_2 group is much shorter in the cation like (1.31 Å) than in the anion like (1.41 Å) molecule. The interstrand hydrogen bond distances are also remarkably different, in line with the different charge present on the 9Me-A monomers. For example, the $NH_2\cdot$OC hydrogen bond distance is 0.3 Å shorter for the "cation"-like 9Me-A base, which is more electrophilic.

According to all of the density functionals employed, AA_{CT}-min is the global minimum of $(9Me\text{-}A)_2\cdot(1Me\text{-}T)_2$ excited states. As shown in Table 2, it is indeed ∼0.1−0.4 eV more stable than the bright excited state minima. Solvent effects significantly stabilize AA_{CT}-min, by ∼0.5−0.7 eV with respect to the gas phase (depending on the density functional and on the basis set adopted), according to *neq* SS-PCM calculations. Furthermore, full equilibration of solvent degrees strongly favors AA_{CT}, due to its much larger dipole moment. In detail, SS-PCM/TD-PBE0/6-31G(d) calculations predict that at the equilibrium level A1-S_B and T1-S_B are more stable by 0.05 and 0.06 eV, respectively, with respect to the nonequilibrium level. On the other hand, AA_{CT} are stabilized by ∼1.7 eV when solvent is fully equilibrated with the excited state density (see Table S2−S5 in the Supporting Information). When considering larger oligomers, one should take into account that the effective polarity of the embedding medium may be reduced by the additional stacked bases. We mimicked this situation running test calculations with a smaller dielectric constant $\varepsilon = 8$ for the solvent, and we proved that also in this case AA_{CT}-min is the global minimum.

In the next section, we document that the A bright state A1-S_B crosses AA_{CT} along the path connecting FC to its minimum, and clearly the same is true also for the corresponding A2-S_B state. Moreover, according to our study on A dimers,[38] A1-S_B and AA_{CT} are strongly coupled at the crossing. The analysis of these results indicate that an effective A1-S_B→AA_{CT} decay occurs within A−T DNA. According to the Kasha's rule AA_{CT}

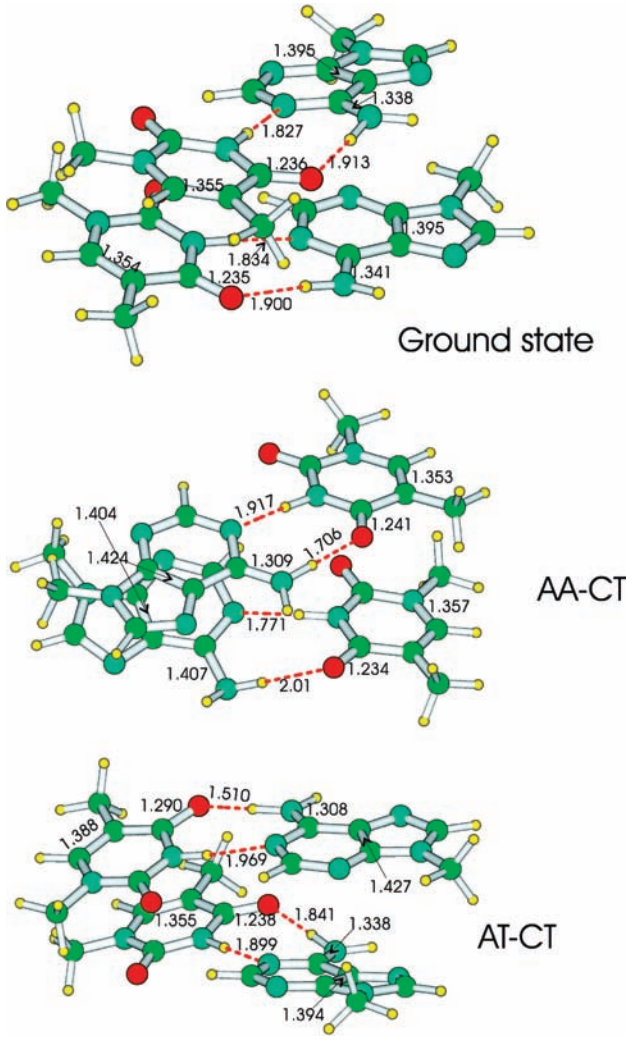

Figure 5. Schematic drawing and selected bond distances (in Å) of the $(9Me\text{-}A)_2\cdot(1Me\text{-}T)_2$ tetramer in the ground state minimum (top), in the minimum of AA_{CT} (middle), and in the minimum of AT_{CT} (bottom). Please note that the orientation of the tetramer is not the same in all of the Figures.

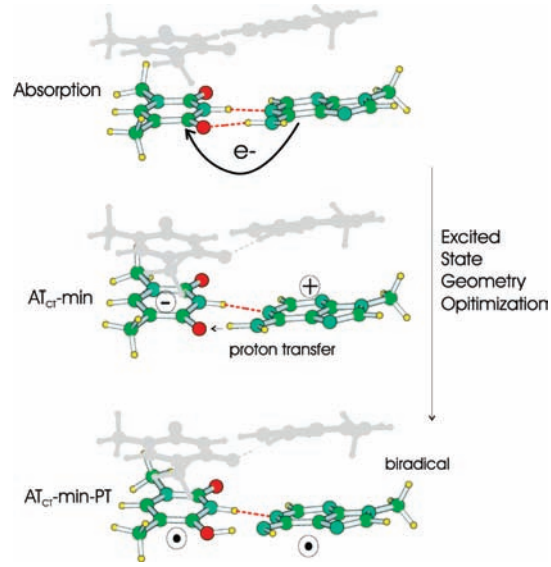

Figure 6. Schematic description of the most significant processes involving the AT_{CT} excited state of $(9Me\text{-}A)_2\cdot(1Me\text{-}T)_2$. The molecules whose Kohn−Sham orbitals are not significantly involved in the electronic transition are depicted in gray.

is therefore the best candidate for the long-living excimer detected in AT DNA. These prediction is in nice agreement with the indications of recent experimental studies,[12] and they confirm our previous results obtained on A single strand.[38,39] The main properties of AA_{CT} in the tetramer closely resemble those predicted for the corresponding state in $(9Me\text{-}A)_2$ dimer,[38] explaining the experimental observation that the long time behavior in $(dA)_{18}$ single strand and in $(dA)_{18}\cdot(dT)_{18}$ double-strand is very similar.[4]

The transition corresponding to the transfer of an electron from a 9Me-A to its hydrogen bonded 1Me-T partner (AT_{CT}) is ∼0.15 eV less stable than AA_{CT} in the FC region (see Figure 2). Geometry optimization of AT_{CT} leads to a flat region of the potential energy surface corresponding to a $9Me\text{-}A^+\cdot 1Me\text{-}T^-$ hydrogen bonded pair (AT_{CT}-min, see Figure 5), as indicated, for example, by the remarkably longer C_5 -C_6 and C_4-O_8 bond distances of $1Me\text{-}T^-$ and the shorter C-NH_2 bond distance of $9Me\text{-}A^+$. Not surprisingly, the interstrand hydrogen $NH_2\cdots OC$ bond distance is also remarkably short, suggesting an incipient proton transfer. LR-PCM geometry optimizations indeed predict a barrierless proton transfer (PT) reaction from 9Me-A to 1Me-T leading to AT_{CT}-min-PT (see Figure 5).

The energy of AT_{CT}-min-PT in gas phase is very close to that of S_0 (∼1.3 eV according to both SS-PCM/TD-M052X/6-31G(d) and SS-PCM/TD-CAM-B3LYP/6-31G(d) calculations) in line with the suggestion of an involvement of PT in the S_0 recovery in GC pairs.[7] These processes are schematically illustrated in Figure 6. However, in aqueous solution, such PT state is destabilized, and it lies 0.2−0.3 eV above the AT_{CT}-min (SS-PCM/TD-M052X/6-31G(d) or SS-PCM/TD-PBE0/6-31G(d) calculations), since it produces a biradical excited state where 9Me-A and 1Me-T are uncharged, whose electric dipole moment is much smaller than the AT_{CT} one (see Table 2). Obviously, since the PT process is ultrafast, a purposely tailored study, explicitly including dynamical solvation effect should be necessary for assessing the PT rate in aqueous solution. However, the above conclusions have been obtained by adopting the nonequilibrium description of the solvent, the most suitable to treat ultrafast phenomena. Full equilibration of solvent degrees of freedom would make the charge separated excited state even more favored over the biradical one.

Data in Table 2 indicate that, in aqueous solution, AT_{CT} -min is less stable than AA_{CT}-min by ∼0.1−0.2 eV. Furthermore, SS-PCM energy paths reported below shows that AT_{CT} does not cross A1-S_B and T1-S_B bright states along the path leading from FC to their minima. As a consequence, an involvement of AT_{CT} in their decay is unlikely.

TD-M052X geometry optimizations provides a similar picture to that obtained by using the minima optimized at the TD-PBE0 level (see Table S5 in the Supporting Information).

Our study allows also excluding any significant involvement in the decay processes of dark states with "intramonomer" $n\rightarrow\pi^*$ character, which instead play some role in the excited state dynamics of the isolated monomers (both A and T).[3,27,32]

Concerning T, the singlet $n\rightarrow\pi^*$ dark state localized on 1Me-T is almost isoenergetic with TT-S_B bright states in $(1Me\text{-}T)_2$ stacked dimer (so that it may be populated by nonadiabatic couplings), but it is significantly destabilized upon base pairing in the double strand.[44] On this ground we can assign to this $n\rightarrow\pi^*$ transition the intermediate state formed with 10/15% yield in $(dT)_{18}$ but absent in $(dA)_{18}\cdot(dT)_{18}$[4]. Analogously, in the

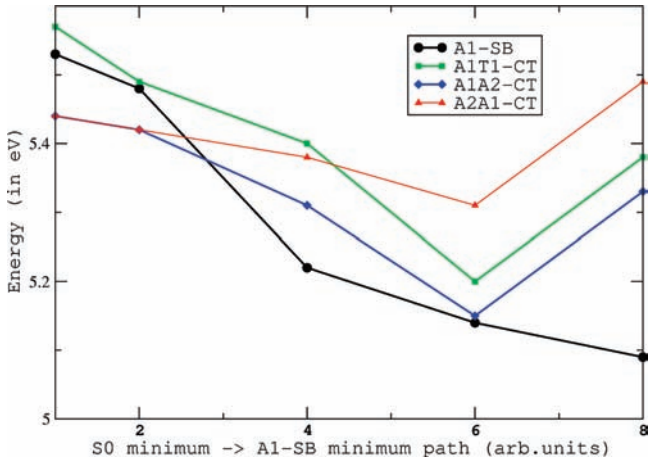

Figure 7. Plots of the energy of the some relevant adiabatic excited states of $(9Me\text{-}A)_2$·$(1Me\text{-}T)_2$ in the region of the coordinate space connecting the FC region and the A1-S_B minimum. The energy is computed at the LR-PCM/TD-M052X/6-31G(d) level. The energies of the CT transitions are shifted to take into account the underestimation of their stability by LR-PCM calculations. The correction for each excited state is obtained as the difference between the VEE computed for that state at the SS-PCM/TD-PBE0 and LR-PCM/TD-PBE0 level in the FC point.

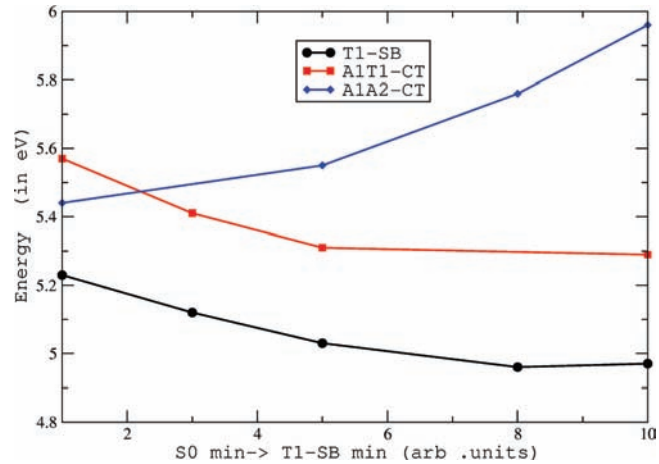

Figure 8. Plots of the energy of the some relevant adiabatic excited state of $(9Me\text{-}A)_2$·$(1Me\text{-}T)_2$ in the region of the coordinate space connecting the FC region and the T1-S_B minimum. The energy is computed at the LR-PCM/TD-M052X/6-31G(d) level. The energies of the CT transitions are shifted to take into account the underestimation of their stability by LR-PCM calculations. The correction for each excited state is obtained as the difference between the VEE computed for that state at the SS-PCM/TD-PBE0 and LR-PCM/TD-PBE0 level in the FC point.

considered tetramer the lowest energy n→π* excited state localized on 9Me-A is significantly less stable than in the isolated monomer.

Also the intrastrand 1Me-T →1Me-T CT state (TT_{CT}) is significantly destabilized upon formation of the double strand. According to SS-PCM/TD-M052X/6-31G(d) calculations, in the FC region TT_{CT} lies only ∼0.1 eV above the most intense bright transition in $(1Me\text{-}T)_2$ stacked-dimer, while it is 0.6 eV less stable than the corresponding absorbing state in the double-strand tetramer. Such a difference is due to the very large dipole moment of TT_{CT}, which is stabilized by the increase of the surface exposed to the solvent, occurring in the single-strand.

It has been proposed that T dimerization, whose mechanism is however still a matter of debate,[62] occurs between stacked nucleobases,[6] and TT_{CT} state is considered its precursor.[63] Therefore, our results might explain why T photodimerization is faster in single strand than in double strand, notwithstanding the fact that base stacking should be more favored in double strand. Nonetheless, other effects might be obviously relevant, like, for example, the possibility that the specific conformational rearrangements needed for photodimerization are more hampered in the double strand. The last considerations clearly show that interpreting results obtained on double strands on the ground of the behavior of single strands can often be misleading.

3.4. One-Dimensional Energy Scan. While only a quantum dynamical study can provide a fully reliable picture of the DNA photophysics, preliminary insights into the dynamical behavior of $(9Me\text{-}A)_2$·$(1Me\text{-}T)_2$ can be gained by selected one-dimensional (1D) energy scans of the lowest energy excited states in the region connecting the FC point to the excited state minima of the bright excited states, that is, A1-S_B (Figure 7) and T1-S_B (Figure 8). Although constraining to few dimensions the motion of the 3N-6 nuclear coordinates involves, of course, some degree of arbitrariness, we think that the selected procedure can give useful qualitative insights. It is indeed clear that in FC region, soon after light absorption, the large majority of the population belongs to the TT-S_B and AA-S_B bright excited states. To ascertain if a population transfer toward other states is possible, it is first necessary to verify if those excited states are sufficiently closer to TT-S_B and AA-S_B in a relevant region of the PES, like that connecting the FC region to their minima.

To this aim, we define collective coordinates by linearly interpolating the internal coordinates of three representative structures (e.g., the FC point and the excited-state minima of T1-SB and A1-SB). In Figure 7 we report the energy of the A1-S_B, two AA_{CT} (A1A2 involves a $9Me\text{-}A_1$→$9Me\text{-}A_2$ charge transfer, A2A1 a $9Me\text{-}A_2$→$9Me\text{-}A_1$ charge transfer) and one AT_{CT} ($9Me\text{-}A_1$→$1Me\text{-}T_1$ CT) excited states. A crossing between A1-S_B and the CT states localized on A strand is predicted, suggesting that a decay to the AA_{CT} states is possible. Although a reliable evaluation of the transition probability is outside our scopes, it is noteworthy that both experiments[4,15] and computations[38] on A single strand predict that the large majority of the excited population in polyA decays to excimer-like states.

The energy scan relative to the path connecting the FC region and the minimum of T1-S_B (see Figure 8) provides different indications. Indeed the energy profile of the T1-S_B is always more stable than the electronic excited states with CT character, and T1-S_B always corresponds to the lowest energy excited adiabatic state. This result suggests the absence of "collective" decay routes through energy-exchange between different nucleobases, supporting the thesis that most of the population of this state goes to the "momomer-like" excited state minimum and, then, directly toward the CI with the ground state. This mechanism is consistent with the fact that, in T derivatives, a vanishingly small energy barrier separates the minimum of the lowest energy bright state from the CI with S_0, in line with its very fast decay (<500 fs).[31]

4. Discussion

DNA is a very complex system and the decay of its excited states is modulated by the subtle interplay of several chemical physical effects. As clearly shown by experiments and computations, each single base can exhibit an intricate excited state

(62) Kwok, W. M.; Ma, C.; Phillips, D. L. *J. Am. Chem. Soc.* **2008**, *130*, 5131–5139.
(63) Boggio-Pasqua, M.; Groenhof, G.; Schafer, L. V.; Grubmuller, H.; Robb, M. A. *J. Am. Chem. Soc.* **2007**, *129*, 10996–10997.

dynamic: several different dark and bright excited states interact and their interaction is modulated by the solvent.[32] Within single and double strands, the number of potentially relevant factors is even larger. Stacking significantly affects the excited state behavior. The bright states localized on each nucleobases can interact not only due to dipolar (excitonic) coupling but, even more, because of the delocalization of the frontier orbitals over multiple bases. Interstrand hydrogen bonding not only affects the stability of the excited states, but provides additional decay channels. Indeed, besides the decay routes present in the isolated monomers (which could also be strongly modulated by the double strand structure), new channels are potentially present in the double strand, involving different kind of excimers, with different degrees of delocalization and of charge transfer character.

Although experiments on A−T DNA highlight that the long-living excited states responsible for the spectroscopic responses we are investigating are singlet (and therefore, we limit our analysis to the study of singlet states), it is clear that triplet excited states are also formed within DNA and they could play a relevant role in modulating the long time dynamics, especially in the nanosecond time-scale.

Double strand fluctuations can also affect the excited state behavior, modulating the number of the bases participating to the excitonic band.[10,11,67] The presence of the phosphoribose backbone, for example, is expected to be very important to study the long time component (time constant ≥50 ps) of the excited state decay, which are likely modulated by significant rearrangement within the double strand geometry.

On the ground of the above considerations, it is not surprising that the excited state decay of DNA double strand exhibits a multiexponential behavior and, often, a significant wavelength dependence: several excited states are involved, each one exhibiting its own peculiar features (emission maxima, for example). Furthermore, it is not easy to get "convergent" results by using different experimental techniques: FU experiments, for example, are more "suitable" to describe bright excited states than dark states and thus it cannot be taken for granted that their results can be "directly" compared with those provided by TA experiments.

Due to the size and the complexity of the systems to be considered (a tetramer is the minimal meaningful model of DNA), in our opinion, no computational method can at the moment reach an "absolute" accuracy, being able to unambiguously assign all of the experimental features. On the other hand, we think that a critical comparison of the available experimental results with the computational results hereby reported provides a consistent picture of the main decay routes for the excited states within A−T DNA, that is, those accounting for the decay of the large majority of the excited state population.

For a poly-A single strand containing more than 15 monomers, we can safely assume that the large majority of the nucleobases are stacked, adopting the B-DNA like structure, not only in $(dA)_n \cdot (dT)_n$ double strands but also in the corresponding single strands (~80% for $(dA)_{18}$[65]). On the other hand, $(dT)_{20}$ single strand cannot be considered an optimal model for the behavior of T strand in DNA double strand, since $(dT)_n$ single strands are very flexible, most T are not stacked and/or are not arranged according to the B-DNA stacking geometry.[66] For example, FU experiments on dT (probe at 330 nm) indicate two decay components with time-constants ~210 fs (68%) and ~1.07 ps.[16] The results obtained for $(dT)_{20}$ are very similar: a biexponential behavior is found, with two time constants at 300 fs (64%) and 1.2 ps.[17]

Our calculations at the FC structure indicate that the absorbing states are delocalized over a single strand (A or T).[44] It is important to note that, for what concerns the absorbing state localized on the A strand, most of the intensity is carried by excited states involving the combination of the HOMO and of the LUMO of the A monomers. They are thus related to the so-called L_a excited state of the monomer (see Supporting Information), which is the most intense transition in the monomer. Experiments provide similar indications: at $t = 0$, the absorbing states are delocalized over multiple bases.[10,11]

4.1. Fastest Excited-State Decay Channel. The geometry optimizations point out the existence of a driving force to localize excitation in single nucleobases. The localization process is barrierless and the double strand helix structure does not induce large geometrical restrains in the excited state minima, which are indeed very similar to those found for the isolated monomers.

A Strand. The emission energy from A1-S_B is similar to the dA one, which, according to experiments, stems mainly from L_a excited state.[15] Interestingly, no significant participation of dimer excited states related to the other weak absorbing excited state in the UV−vis spectrum of the monomer (the so-called L_b excited state) is predicted in the decay of A-S_B. On the ground of our results, we could thus expect that, in the absence of additional decay channels, the emission properties of polyA single strand are very similar to those of isolated A. The results of fluorescence upconversion experiments on $(dA)_n$ are fully consistent with the picture provided by our calculations. Let us start by comparing the experimental results obtained on $(dA)_n$ single strand: they are usually fitted by using expression of the type:

$$S(t) = a_1\exp(-t/\tau_1) + a_2\exp(-t/\tau_2) + ...a_n\exp(-t/\tau_n) \quad (1)$$

where S is the time dependent signal, corresponding to the $S_1 \rightarrow S_0$ fluorescence in FU experiments, and to the $S_1 \rightarrow S_n$ excited state absorption (ESA) in TA experiments (although other processes such as hot ground-state absorption and stimulated emission can come into play). The value of the a_n weights of the different components cannot be considered an exact measure of the excited population undergoing the corresponding decay-route, since in principle different regions of the excited state surface could have different emission or ESA intensities, introducing a modulation of the measured signal that is independent of population transfers. In any case, (as shown in Table 1), all the experimental studies performed on $(dA)_n$ indicate that, although a noticeable wavelength dependence and different components are present (the slowest ones are discussed below), an ultrafast ($\tau \approx 400-600$ fs) decay channel exists and it accounts for most of the emission from $(dA)_n$ excited states (the coefficient of the ultrafast decay channel is >0.75). According to Kerr-Gated time-resolved fluorescence (KTRF) experiments,[15] the maximum (310 nm, see Table 1) and the

(67) (a) Starikov, E. B. *Philos. Mag. Lett.* **2003**, *93*, 699–708. (b) Lewis, J. P.; Cheatham, T. E., III; Starikov, E. B.; Wang, H.; Sankey, O. F. *J. Phys. Chem. B* **2003**, *107*, 2581–2587.
(65) Dewey, T. G.; Turner, D. H. *Biochemistry* **1979**, *18*, 5757–5762.
(66) (a) Martinez, J. M.; Elmroth, S. K. C.; Kloo, L. *J. Am. Chem. Soc.* **2001**, *123*, 12279. (b) Johnson, A. T.; Wiest, O. *J. Phys. Chem. B* **2007**, *111*, 14398–14404. (c) Law, Y. K.; Azadi, J.; Crespo-Hernandez, C. E.; Olmon, E.; Kohler, B. *Biophys. J.* **2008**, *94*, 3590–3600.

line-shape of the fastest component signal in $(dA)_{20}$ is very similar to that of A and, specifically, to the component that can be ascribed to the L_a state ($\tau = 0.13$ ps, fluorescence maximum at 307 nm).

In the following we label the state corresponding to this component as M_A (monomer-like A). Our calculations, indicating a barrierless localization process, show that this latter result is fully consistent with the presence of "delocalized" absorbing states.[10,11] Finally, our picture (delocalized absorption/localized emission) is consistent with fluorescence anisotropy experiments.[18]

FU experiments can only document that a significant component of the fluorescence signal decays on a subps time scale, but cannot really individuate the decay mechanism, that is, if the decay implies ground state recovery or simply a population decay to a dark state. On the ground of their experimental results, both Kwok et al.[15] and Kohler et al.[4] suggest that the bright state of stacked A monomers mainly decays to a long living excimer state and that only unstacked molecules can exhibit a ground state recovery similar to that of the isolated monomers. As discussed below, our results are not in contradiction with this picture. However, we notice that according to the Kohler's estimate, the excimer population is always smaller (by at least ~15%) than that of the stacked bases population, both in multimers and in dimers.[12] As a consequence (also in analogy with what found for T strand, see below), we can expect that also within polyA (single- and double-strand) some stacked A bases can decay to the ground state on a subps time-scale via a monomer-like mechanism. Actually, subps excited state decay components have been documented almost in all the homopolynucleotide single strands (both purine and pyrimidine).[5]

A−T Double Strand. Our calculations indicate that the same barrierless localization process described for A strand, occurs for the excited state localized on T strand and that the properties of T1-S_B are similar to that of dT. On this respect, it is significant that the experimental emission spectra of $(dT)_n \cdot (dA)_n$ is almost superimposable to that of isolated (dT), confirming that excited state minima are not significantly affected by the DNA double strand.[18] Furthermore, the maximum of the measured spectra changes by only 300 cm^{-1} in the first 2.2 ps (the experimental error is ± 100 cm^{-1}). Also in this case, although a wavelength dependence is found (vide infra), the main component of the fluorescence decay exhibits an ultrafast decay (it reaches a maximum after 0.2 ps), as shown by the results reported in Table 1.

Many factors give account of the experimental finding that the contribution of A to the emission of $(dA)_n \cdot (dT)_n$ is much smaller than that of T. Our calculations (independently of the adopted functional) predict indeed that the potentially emitting states T1-S_B and T2-S_B have more stable minima than A1-S_B and A2-S_B (see Figure 3). From the data in Table 2, the energy gap ranges from 0.04 to 0.19 eV. T emission is thus favored over A emission. This conclusion is strengthened by the fact (documented in Figures 7−8) that during the system motion on A-S_B toward its minimum a cross with AA_{CT} does occur, enabling a A-$S_B \rightarrow AA_{CT}$ population transfer, while this does not happen for T1-S_B, whose minimum is more likely reached, increasing the fluorescence yield.

The similarity of the TR decay in $(dA)_{20} \cdot (dT)_{20}$ and in TMP (thymidine-monophosphate), especially in the subps time component,[18] together with the resemblance of their steady state spectra, suggests that a significant percentage of the excited state population on the T strand can follow the same decay path predicted for the isolated monomer, reaching a conical intersection (CoI) with S_0 by out-of-plane motion of the methyl substituent.[24,31,32] The steric hindrance of the double strand can increase the energy barrier associated to this path, giving account of the faster ground state recovery of the monomer.

4.2. Slow Decay Channels of the A Single Strand. KTRF experiments on $(dA)_{20}$ indicate that, besides the subps component discussed above, two long-time components are present.[15] The first (E1) is characterized by a time-constant of ~5 ps, and according to KTRF experiments it exhibits a fluorescence maximum at ~350 nm. Although it contributes to the fluorescence signal much less than the subps decay channel (see Table 1 and ref 15), its longer lifetime gives account of the shift of the fluorescence maximum of polyA with respect to A. The second component (E2) decays with a time constant in the ~150 ps range and it gives rise to a weak emission maximum at 390 nm. Those long living states have been assigned to excimers and they have been also related to the slowest decay channels (lifetime $\approx$ 100 ps) evidenced in the A−T double strand by TA experiments.[4] Similar results are obtained by Schwalb and Temps[5] monitoring the fluorescence at 350 nm of $(dA)_{20}$ by TR FU experiments: together with an ultrafast decay channel, two additional slower components are present, with τ 5.80 and 97 ps, respectively.

In a very recent contribution, Serrano-Andrés et al. have assigned these transitions to "neutral" excimers, which exhibit a stacking geometry significantly different with respect to the B-DNA, with perfect face-to-face arrangement and significantly smaller interbases distances (<3 Å).[40] These excited states are related to the lowest-energy bright transitions of A monomer, which at the CASPT2 level correspond to L_b excited state[27] and not to L_a, which is instead the excited state carrying most of the oscillator strength in the UV−vis spectra of A.[1,27] The formation of "dark" excimers within stacked molecules is likely. We have seen that in the absorption spectra of the dimer and the tetramer one of the transitions, namely the one on the redwing of the spectrum, resulting from the antisymmetric combination of the monomer bright transitions, is almost dark.[44] In our previous study on A dimer we have localized the minimum of this excimer, with the electronic excitation always almost equally delocalized over the two monomers.[38] However, the emission energy of this excited state is larger than that of the localized A-S_B excited state deriving from the bright transition. Actually, this result can be due to the fact that we have always kept the stacking orientation frozen to that of B-DNA. In fact, a strongly red-shifted emission energy can be obtained by a significant destabilization of the ground state, for example admitting that the stacking geometry of the excimer is significantly different from that of S_0.

On this respect, it is important to remember that Kwok et al. interpret their KTRF experiments by invoking an ultrafast formation of the E1 excimer, assigning a 0.4 ps time constant to the $M_A \rightarrow$E1 decay.[15] In our opinion, such an ultrafast process can be hardly reconciled with large variation of the stacking geometry. This process would surely involve also the backbone, whose conformation should change in order to avoid too unfavorable steric hindrances. From the dynamical point of view, it is reasonable to assume that such large amplitude motion, besides their intrinsic energetic cost, cannot occur on an ultrafast time scale (i.e., ~500 fs).

Additional difficulties arise if we accept the hypothesis that E2 corresponds to the excimer state responsible of the ~100 ps decay according to TA experiments of Kohler et al.[4] in $(dA)_{18}$

and $(dA)_{18}\cdot(dT)_{18}$ (vide infra). In fact, not only is this latter excited state formed on ultrafast time-scale (<1 ps according to Kohler[12]) but it exhibits very similar features both in the single and in double strand. It is not likely that a process involving a strong perturbation of the stacking geometry would not be affected by the presence of the hydrogen bonding network of the double-strand.

We are thus convinced that inclusion of the backbone is a prerequisite for a reliable modeling of the slower decay channels. On the other hand, on the ground of the available experimental and computational results, different explanation of the origin of E1 and E2 excited states are possible, without implying dramatic structural rearrangements. The first possibility is that both E1 and E2 excited states has a substantial CT character: the former exhibiting a stacking geometry similar to that of the B-DNA, the latter involving a more substantial structural rearrangement. Within the single strand the emission energy of intrastrand CT states are characterized by a strongly red-shift emission energy with respect to that of the monomer also within a B-DNA stacking geometry. For example, SS-PCM/TD-CAM-B3LYP calculations[39] indicate that emission from the AA_{CT} minimum is ∼0.4 eV red-shifted with respect to that of the bright state, in the nonequilibrium time-regime. This difference is larger than 1.5 eV when the solvent equilibrium time-regime is used (long-time limit). It is clear that, when dealing with CT excited states, strongly red-shifted emission are fully compatible with stacking geometries similar to that adopted within single and double A−T DNA strands.

A second possible interpretation of the multiexponential behavior of the Fluorescence decay in $(dA)_n$ single strand is based on the finding that isolated nucleobases can also exhibit a biexponential fluorescence decay.[15,31,36] Interestingly, KTRF experiments evidence indeed that in the monomer, besides the M_A-like ultrafast decay channel, an additional component is present: its emission maximum (around 350 nm) is the same of the E1 state, although its lifetime is 1 order of magnitude shorter. It is thus possible that E1 is representative of a decay channel present already in the monomer, whose lifetime and population increases within stacked systems. Actually, a recent paper on Guanine[36] indicates that nonplanar regions of the excited-state PES, those leading to the CoI with the ground state, are characterized by red-shifted emission with respect to the steady-state fluorescence maximum. Protonation of the guanine ring leads to the formation of the real "nonplanar" minimum on the excited state surface and strongly increases the lifetime of this component. As a consequence, the steady-state fluorescence spectrum of protonated guanine is strongly red-shifted with respect to the neutral monomer.[36] Analogously, we can think that stacking can make more difficult the out-of-plane motion leading the excited states (deriving either from L_a and/or L_b) toward the CoI with the S_0,[27] increasing the contribution of strongly nonplanar region of the PES to the emission spectrum. Actually, emission from nonplanar geometry is expected to be significantly weaker and red-shifted with respect to that stemming from the FC region.

4.3. Slow Decay Channels of the A−T Double Strand. TA experiments indicate that a decay channel with time constant $\tau = 0.8$ ps is present both in $(dA)_{18}$ and in $(dA)_{18}\cdot(dT)_{18}$ oligonucleotides.[4] However, a large part of the excited state population decays to a state ($E2_{TA}$) exhibiting a much longer lifetime, with a time constant (τ) ≈ 120 ps.[4] As we have anticipated above, the formation of $E2_{TA}$ is fast (it likely occurs within 1 ps after the excitation) and effective (it involves ∼65% of the excited state population).[4] Moreover we know that its experimental behavior in $(dA)_{18}$ and $(dA)_{18}\cdot(dT)_{18}$ is very similar.

Our calculations indicate that the lowest-energy excited-state minimum corresponds to AA_{CT}. The energy difference between AA_{CT}-min and the minima of the bright excited states (∼0.2−0.4 eV) is at the limit of the expected accuracy of our method. On the other hand, it must be highlighted that CT states are likely disfavored by our computational approach, using nonequilibrium solvation regime, and preventing significant variation of the stacking geometry. Furthermore, all of the main features of AA_{CT} are fully consistent with the properties revealed by the experiments, like similarity between the behavior found in single and double strands and the isotope effect exhibited by its lifetime.[4] Our calculations give very strong evidence that the slow components (>1 ps) are associated with an AA_{CT} excimer localized on A strand, (see Figure 3) involving the CT transition between two stacked A. This prediction fully agrees both with that provided by the experimental results on the different stacked dinucleosides[12] and also with the indications of a very recent study on $(dA)_{20}\cdot(dT)_{20}$.[20]

Although we have shown that AA_{CT} state is present both in single and double strands and that it could be related also to long-living $E2_{TA}$ state detected in dA single strands, it cannot be taken for granted that the long living states evidenced by FU experiments on $(dA)_{18}$ (E1 and E2) are the same found within A−T DNA.

First, it is important to highlight that the most recent FU experiments on the A−T double strand do not show any evidence of a ∼100 ps component. The slowest component is 16 ± 4 ps according to Schwalb, with a very small coefficient.[5] Markovitsi et al. monitored the emission at different wavelengths, and they found that the slowest time-component in $(dA)_{20}\cdot(dT)_{20}$ has a time constant of ∼2−5 ps. Also when studying emission at 420 nm, where the contribution from E2 should be maximum, the longest time constant is 6.2 ps, with a coefficient of 0.19. It is obviously possible than the weak emission from E2 is masked within A−T DNA by the T fluorescence. On the other hand it is meaningful that no clear evidence for the presence of a ∼100 ps emitting state has been documented until now for A−T DNA. More in general while the TA spectra of $(dA)_{18}$ and $(dA)_{18}\cdot(dT)_{18}$ are very similar, the FU spectra of single and double strand are rather different, as shown by the results reported in Table 1.

Our results prove that the possible decay route through a A→T PT following a CT-intermediate between A and T, which has been claimed to be dominant for GC pairs in gas-phase,[7,9] is strongly disfavored in aqueous solution due to the quenching of the electric dipole of the AT_{CT} state by PT. On the other hand, the stability of AT_{CT} is not remarkably smaller than that of AA_{CT}. As a consequence, solvent degrees of freedom could increase the population of interstrand CT states at the helix terminus, where the better exposition to the solvent (with respect to that felt in the core of the double strand) should stabilize AT_{CT} state due its very large dipole moment, especially within a long-time (equilibrium) regime for solvation dynamics.

The present study thus definitively shows that for A−T DNA base-stacking plays a much more relevant role than base-pairing in modulating the excited state decay.

In AA_{CT}-min an "anion-like" 9Me-A monomer is stacked with a "cation-like" 9Me-A monomer, leading to a significant variation of the interstrand hydrogen bond geometry with respect to S_0 (see Figure 4). On a longer time scale this would likely

induce significant geometry rearrangements within the double strand, which would loose its regular and "symmetric" stacking geometry. It is not yet possible to provide indications about the nature of this geometry rearrangement, since larger strand portions should be included in the calculations. However, the existence of a fully relaxed CT minimum could in principle be relevant to the $E2_{TA}$ decay channel: the slowness of the decay (>100 ps) is indeed compatible with a significant conformational rearrangement within the DNA strand. On the other hand, the close similarity between the decay in double and single double strands and the correlation between the decay rate and the energetics of the CT process[12] suggest that the basic mechanism for the exciplex decay involves a charge recombination process.

When considering more complex oligomers than A−T DNA, we can foresee that a key factor ruling the most effective decay channels is the relative stability of the different intrastrand and interstrand CT excimers. It is thus possible to explain the experimental results obtained on single strand dimers formed by different nucleobases.[5] Since the G HOMO is less stable than the A one, we expect that G^+-A^- CT states are more stable than A^+-A^- ones.

In the real DNA system, we cannot exclude that the decay routes involve also interstrand CT states between G-C pairs. Actually, in agreement with previous studies,[9,58] we find (see Supporting Information) that the G→C CT state is relatively more stable than the corresponding A→T state. On the other hand, our calculations suggest that also for G→C CT solvent effects could make more difficult the PT process, since it would lead to large decrease of the excited state dipole moment. Actually, recent experiments on (GC)·(GC) double strands in aqueous solution, although indicating that the excited state decay is faster than for the isolated monomers, do not reveal any signature of ultrafast interstrand PT processes.[22] Furthermore, TA experiments on GC duplexes in water suggest that the ground state recovery occurs 10 times more slowly than for the isolated nucleotides and that the loss of fluorescence signal is likely due to the fast decay of the bright state populations to under-lying dark states.[23]

Although a specific theoretical study on GC oligomers would be necessary for assessing the involvement of G→C CT states, these results highlight that solvent significantly modifies the excited state dynamics and that its inclusion in the theoretical model is fundamental for interpreting experiments on DNA.

5. Conclusions

As discussed in the present contribution, the excited state decay of DNA can be in principle modulated by several different factors, whose inclusion within a single theoretical/computational model is a very challenging task. Taking into account double strand fluctuations, which modulate the number of the bases participating to the excitonic band,[10,11] and including in the calculations water molecules,[64] metal ions, and a larger number of nucleobases could thus improve our model, when it will be computationally feasible. Furthermore, when dealing with a complex system as DNA in solution, any computational approach suffers from intrinsic limitations and possible sources of inaccuracy. Also when the computational accuracy is carefully checked, errors of a few tenths of eV are probably unavoidable, and in some cases, they could provide a qualitatively wrong picture of the decay mechanism. Finally, it is always important to remember that only a fully quantum dynamical treatment can be directly compared with time-resolved experiments. Some of the features evidenced by the experiments could have a "purely" dynamical origin, without being related, for example, to the interaction between different excited states. This conclusion has already been proven true in "isolated" chromophores[68] and, when dealing with a multichromophore system as DNA, unexpected dynamical features could be present.

Notwithstanding the above discussion, we think that the results hereby reported provide encouraging indications about the potentialities of first principle quantum mechanical methods in the treatment of the excited state decay of DNA double strand. In fact, for the first time, we have located the minima of the lowest energy excited states of a "realistic model" of A−T DNA, the $(9Me\text{-}A)_2\cdot(1Me\text{-}T)_2$ stacked tetramer in aqueous solution. The good agreement between our predictions (robust with respect to the adoption of different functionals, basis sets and time-regimes for the solvent description) and the available experimental results indicates that our model captures the essential physics of the absorption and emission processes of A−T DNA, especially for what concerns the fastest components, which are ruled by the nucleobase's intramolecular degrees of freedom. Confirming the results obtained studying A single strand,[38,39] the most significant dynamical processes (from the instant of absorption to the quenching of emission) thus occur within stacked nucleobases dimers, in nice agreement with the most recent experimental indications.[12]

While the absorbing bright states are delocalized over A and T strands, our calculations predict that barrierless/ultrafast localization of the excitation on single monomer are active both in single and double strand. This result gives account also of the experimental finding that, even in very strongly stacked systems, the early (0−2 ps range) fluorescence decay is very similar to that found in the monomer and most of the fluorescence intensity exhibits "monomer-like" features.

According to our computations, monomer-like fluorescence decay channels are thus not an exclusive feature of unstacked bases. For A strands, the transfer to dark intrastrand excimers is predicted to be very effective, therefore providing an additional decay channel for the fluorescence signal. For the bright excited states localized on T, the decay to excimer states should not be a dominant process. Although only a purposely tailored study can assess how the deactivation of A1-S_B and T1-S_B is affected by the double strand, our calculations suggest that, after localization, the T1-S_B population should decay to the ground state through a "monomer-like" CoI with S_0.[24,32] Within a double-helix, this process should be characterized by a larger barrier than for the isolated monomer, giving account of the slower decay rates of this monomer-like component.

For what concerns the slower decay channels, our calculations indicate that also within a double strand the formation of dark excimer between two stacked A is a strongly favored process. Especially in their minima, these excimers exhibit a clear-cut CT character and they constitute the absolute excited state minimum in A−T DNA. Neutral excimers have been also predicted in A single strand,[38,40] and we cannot exclude that for strongly distorted stacking geometry (especially in the single strand) their stability could be comparable to that of the CT states. However, the results obtained on dinucleosides[12] and the

(64) Conwell, E. M.; McLaughlin, P. M.; Bloch, S. M. *J. Phys. Chem. B* **2008**, *112*, 2268–2272.

(68) (a) Olivucci, M; Lami, A; Santoro, F. *Angew. Chem., Int. Ed.* **2005**, *44*, 5118. (b) Santoro, F.; Lami, A.; Olivucci, M. *Theor. Chem. Acc.* **2007**, *117*, 1061.

similarity of the behavior exhibited by these excimers within single and double strands[4] find the most natural explanation in our prediction that they have a substantial CT character. Interstrand CT states play instead a less significant role in the excited state decay. Furthermore, especially in aqueous solution, interstrand PT is not predicted to be a key mechanism for the ground state recovery.

In summary, our study provides a comprehensive and unitary description of the behavior of the lowest excited states of A−T DNA, allowing a consistent explanation for the most significant experimental features and identifying the states responsible for the different lifetime components evidenced by time-resolved experiments. For the first time, the absorption[44] and emission spectra of DNA-like systems have been reproduced by first principle calculations on realistic models in solution, allowing a significant step toward a deeper understanding of the photodeactivation mechanism of DNA.

Supporting Information Available: Additional considerations on the adopted computational approach; tables reporting a more detailed description of the properties of the relevant minima of the PES; description of the lowest energy excited states of the monomers; Cartesian Coordinates of the most relevant minima. Complete ref 47. This material is available free of charge via the Internet at http://pubs.acs.org.

JA904777H